Electronic Supplementary Material (ESI) for ChemComm.
This journal is © The Royal Society of Chemistry 2022

Engineering nickel vacancies in NiCo LDHs nanoarrays accelerates hydrogen evolution and oxygen evolution reactions

Wenjun He, [a] Da Cao, [a] Dongqin Ma, [a] Ying Li, [a] Cong Chen, [a] Limin Liang [a], * and Hui Liu [a], *

[a] Key Laboratory of Special Functional Materials for Ecological Environment and Information (Hebei University of Technology), Ministry of Education, Tianjin 300130, People's Republic of China.

Experimental section

Materials.

$Ni(NO_3)_3 \cdot 6H_2O$, $Co(NO_3)_3 \cdot 9H_2O$, $ZnCl_2$, NaOH, NH_4F, urea and ethyl alcohol were provided by Aladdin without further purification. Carbon cloth (CC) was purchased from Wuhan Instrument Surgical Instruments business. Pt/C, IrO_2 and Nafion were bought from Sigma Aldrich. Deionized water (DIW) was used throughout the experiments.

Synthesis of Zn-NiCo LDH/CC and NiCo LDH/CC.

Firstly, 2.5 mmol $Ni(NO_3)_3 \cdot 6H_2O$, 0.25 mmol $Co(NO_3)_3 \cdot 9H_2O$, 0.125 mmol $ZnCl_2$, 4 mmol NH_4F and 10 mmol urea were dissolved in 35 mL deionized water. After stirring until complete dissolution, the solution was transferred to an autoclave. Then, two pieces of CC (1×3 cm^2) were put into the autoclave and reacted at 120 °C for 6 h. Finally, the samples were washed several times with ethanol and water, and dried in a vacuum oven at 60 °C to obtain Zn-NiCo LDH/CC. NiCo LDH/CC was prepared by the same hydrothermal method, except that $ZnCl_2$ was not added.

Synthesis of NiCo LDH-V_{Ni}/CC.

A piece of Zn-NiCo LDH/CC was placed in a 2 M NaOH solution and soaked for 1 h. Then the sample was taken out and washed with DIW for several times. Finally, it was dried in a vacuum oven at 60 °C to gain NiCo LDH-V_{Ni}/CC.

Structural Characterization.

X-ray diffraction (XRD) was performed on Bruker AXS diffractometer with Cu-Kα radiation. Scanning electron microscopy (SEM) as well as energy dispersive spectroscopy (EDS) were observed on Zeiss Gemini 300. Transmission electron microscopy (TEM) images were acquired on FEI Tecnai F20. The X-ray photoelectron spectroscopy (XPS) spectra were carried out on Thermo Scientific K-Alpha.

Electrocatalytic measurements.

OER and HER electrocatalytic activity measurements were performed in 1M KOH solution using an electrochemical workstation (CHI660E) with a standard three-electrode system, which were working electrode (samples), counter electrode (carbon rod) and reference electrode (Hg/HgO). Convert all potentials to reversible hydrogen electrodes (RHE) according to the Nernst equation: $E_{RHE} = E_{Hg/HgO} + 0.098 + 0.059\ V \times pH$. Line Sweep Voltammetry (LSV) was tested at 2 mV/s with IR compensation. Double-layer capacitance (C_{dl}) was gained through CV measurement, which was scanned at different scan rates from 5 mV/s ~ 150 mV/s. Electrochemical impedance spectroscopy (EIS) was performed at -0.2 V (RHE) for HER and 0.25 V (RHE) for OER with an AC amplitude of 5 mV in the frequency range of 100 kHz to 0.1 Hz. Long-term stability was tested for 3000 cycles by CV at 100 mV/s.

DFT Calculations.

Density functional theory (DFT) calculations were performed using the Vienna Ab initio Simulation Package (VASP). [1] Electron exchange and correlation interactions were described using a generalized gradient approximation (GGA) with a Perdew-Burke-Ernzerhof (PBE) functional. [2] The 3 × 3 × 1 Monkhorst–Pack sampling of the Brillouin zone is used for integration and the cutoff energy was 450 eV. Geometric optimization was performed using the conjugate gradient method with convergence thresholds set at 10^{-5} eV for energy and 0.02 eV $Å^{-1}$ for force. The crystal plane of NiCo LDH-V_{Ni} used is the (003) plane, and the vacuum layer was 15 Å. The geometric parameters of the supercell model are a=9.09760 Å, b=5.35180 Å, c=24.98380 Å.

The adsorption Gibbs free energy of hydrogen is defined as by

$$\Delta G_{H*} = \Delta E_{H*} + \Delta ZPE - T\Delta S,$$

where ΔE_{H*} is the adsorption energy of H atom calculated by $\Delta E_{H*} = E_{H*} - E_{*} - \frac{1}{2}E_{H_2}$, ΔZPE is the difference in zero-point energy, and ΔS represents the entropy change of H* adsorption. ΔZPE–TΔS=0.24 eV. [3] And for OER, the Gibbs free energy diagrams of four elementary reaction steps are obtained based on the above Gibbs free energy equation. The adsorption energies of intermediates OH*, O* or OOH* are calculated by

$$\Delta E_{OOH*} = E_{OOH*} - E_{*} - (2E_{H_2O} - \frac{3}{2}E_{H_2})$$

$$\Delta E_{O*} = E_{O*} - E_{*} - (E_{H_2O} - E_{H_2})$$

$$\Delta E_{OH*} = E_{OH*} - E_{*} - (E_{H_2O} - \frac{1}{2}E_{H_2})$$

where E_{OOH*}, E_{O*} and E_{OH*} are the energies of OOH, O and OH adsorption on the catalyst surface, and E_* is the energy of the catalysts, and E_{H_2O} and E_{H_2} are the energies of H_2O and H_2 molecules in the gas phase. ΔZPE is obtained by calculating the vibration frequency using DFT calculation.

The detailed calculation results are shown in the following table:

Catalysis	ΔG_{H2O*}	ΔG_{H*}		U = 0 V		
		Ni site	Co site	ΔG_{OH*}	ΔG_{O*}	ΔG_{OOH*}
NiCo LDH	-0.15	1.12	0.84	--	--	--
NiCo LDH-V_{Ni}	-0.42	0.51	0.22	--	--	--
NiCoOOH	--	--	--	2.59	3.49	4.51
NiCoOOH-V_{Ni}	--	--	--	1.26	2.33	4.25

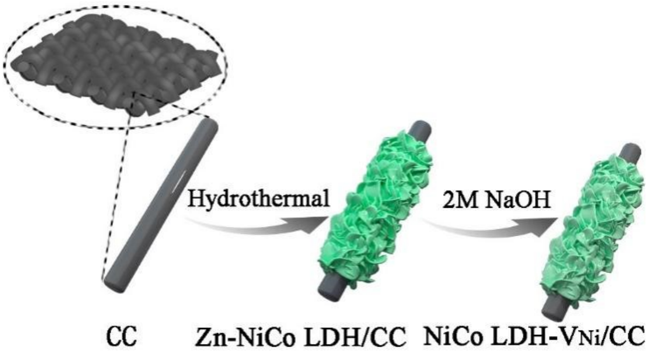

Fig. S1. Schematic showing the synthesis of NiCo LDH-V_{Ni}/CC.

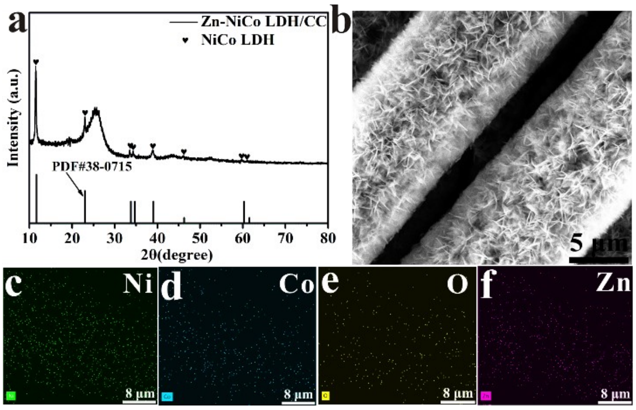

Fig. S2. (a) XRD pattern, (b) SEM image and (c-f) the element mapping of Zn-NiCo LDH/CC.

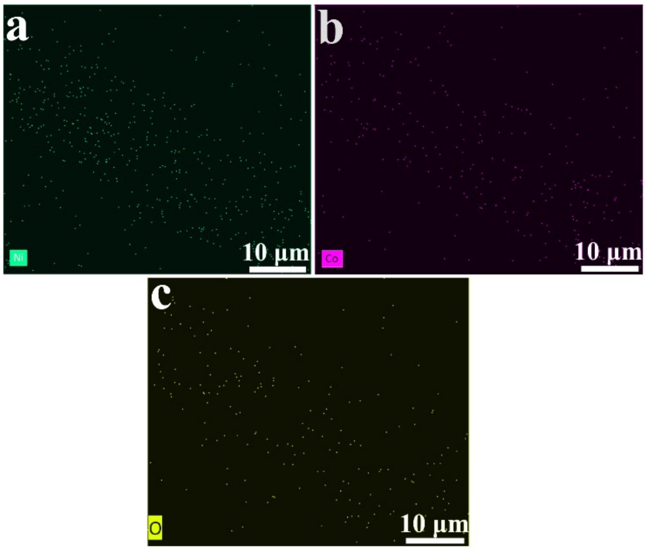

Fig. S3. The element mapping of NiCo LDH-V_{Ni}/CC.

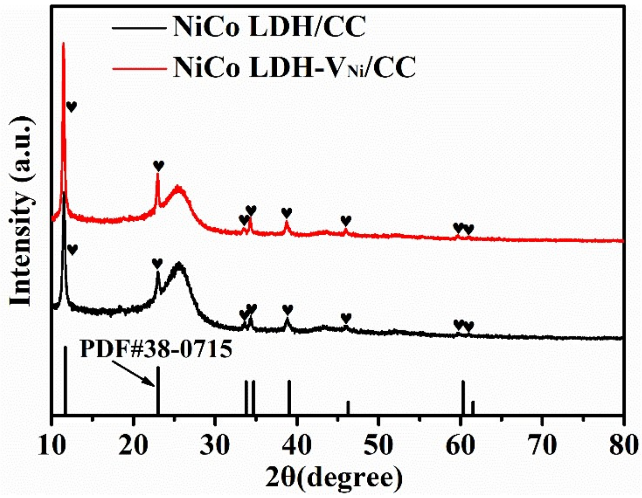

Fig. S4. XRD patterns of NiCo LDH/CC and NiCo LDH-V_{Ni}/CC.

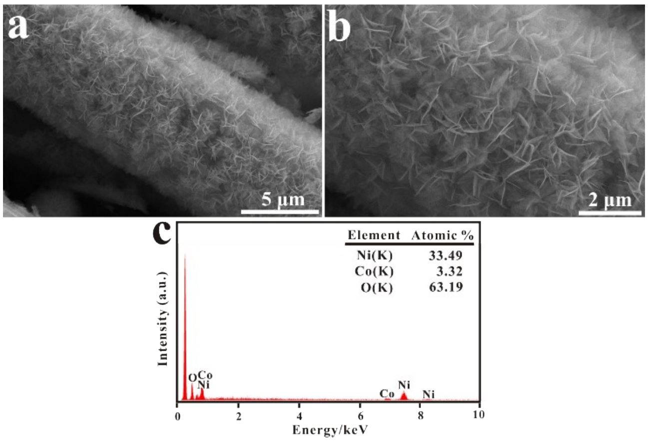

Fig. S5. (a-b) SEM images and (c) EDS spectra of NiCo LDH/CC.

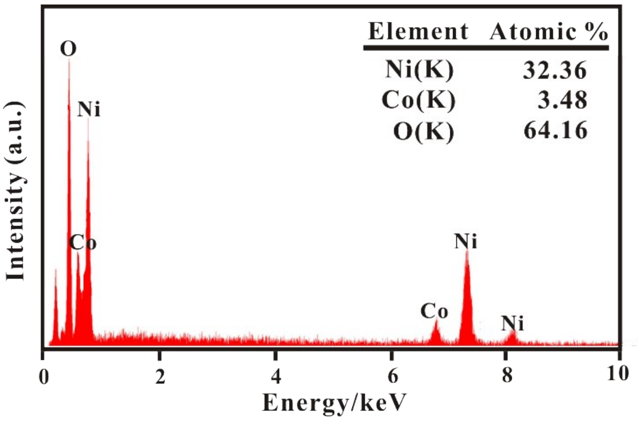

Fig. S6. EDS spectra of NiCo LDH-V_{Ni}/CC.

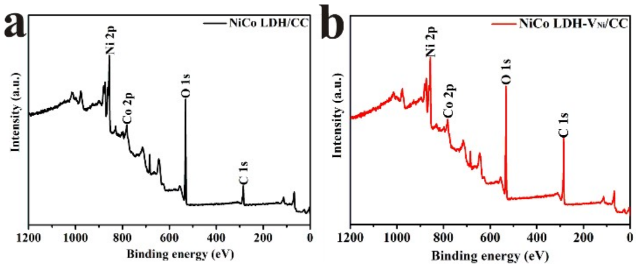

Fig. S7. XPS full spectra of (a) NiCo LDH/CC and (b) NiCo LDH-V_{Ni}/CC.

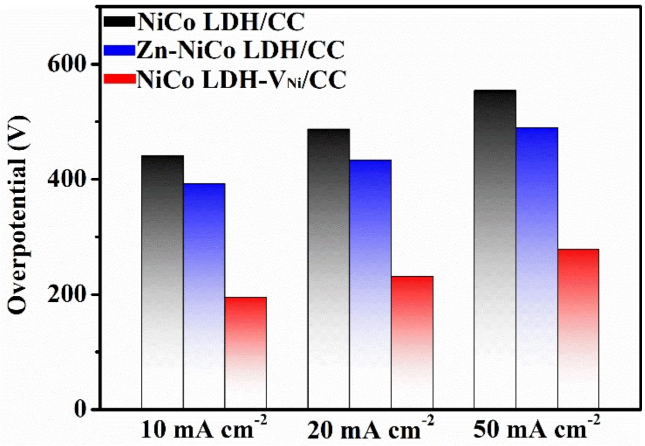

Fig. S8. Comparison of overpotentials of the catalysts at 10, 20 and 50 mA cm^{-2} for HER.

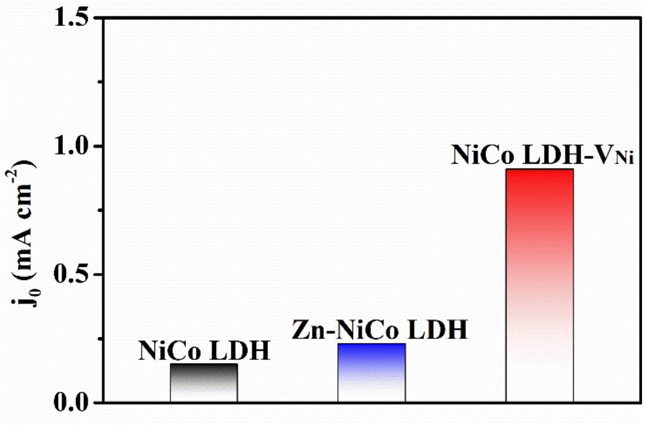

Fig. S9. Exchange current density of NiCo LDH/CC, Zn-NiCo LDH /CC and NiCo LDH-V_{Ni}/CC for HER.

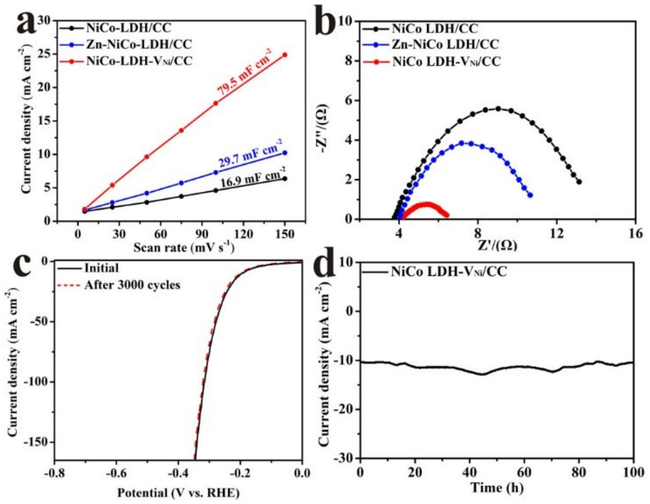

Fig. S10. (a) C_{dl} values and (b) EIS results of NiCo LDH/CC, Zn-NiCo LDH/CC and NiCo LDH-V_{Ni}/CC. (c) LSV curves of NiCo LDH-V_{Ni}/CC before and after 3000 CV tests. (d) Chronoamperometric stability of NiCo LDH-V_{Ni}/CC for HER at a current density of 10 mA/cm^2.

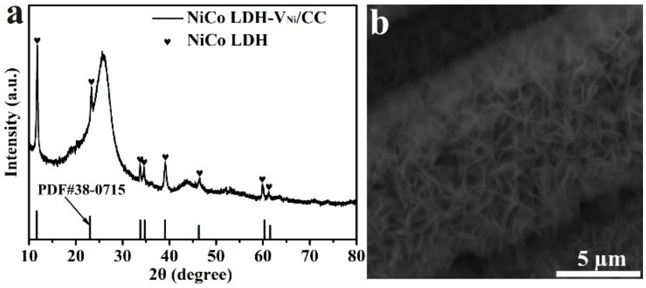

Fig. S11. (a) XRD pattern and (b) SEM images of NiCo LDH-V_{Ni}/CC after HER stability test for 100 h.

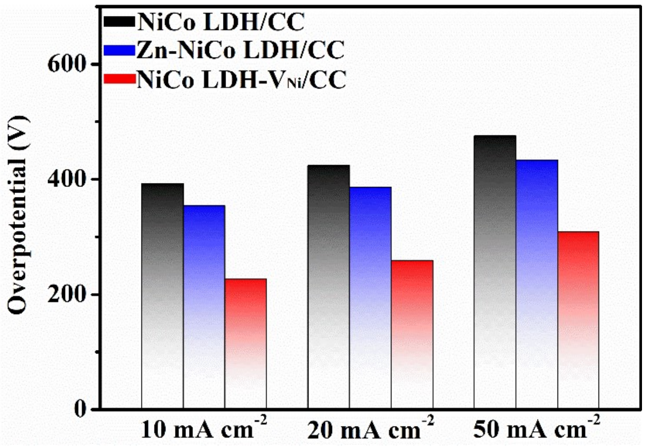

Fig. S12. Comparison of overpotentials of the catalysts at 10, 20 and 50 mA cm^{-2} for

OER.

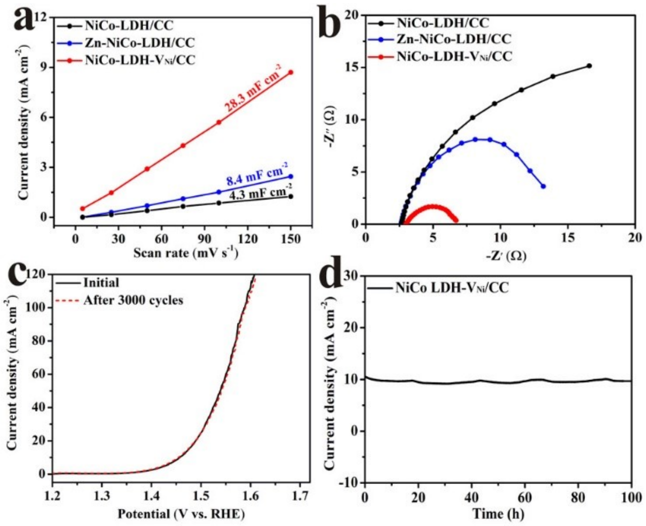

Fig. S13. (a) C_{dl} values and (b) EIS results of NiCo LDH/CC, Zn-NiCo LDH/CC and NiCo LDH-V_{Ni}/CC. (c) LSV curves of NiCo LDH-V_{Ni}/CC before and after 3000 CV tests. (d) Chronoamperometric stability of NiCo LDH-V_{Ni}/CC for OER at a current density of 10 mA/cm^2.

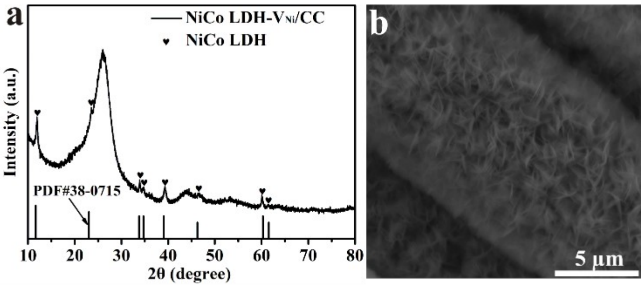

Fig. S14. (a) XRD pattern and (b) SEM images of NiCo LDH-V_{Ni}/CC after OER stability test for 100 h.

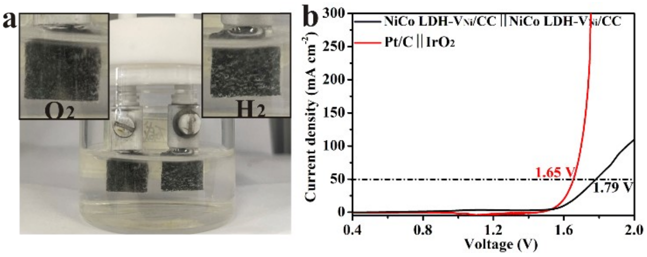

Fig. S15. (a) Image of overall water splitting for NiCo LDH-V_{Ni}/CC||NiCo LDH-V_{Ni}/CC electrode pairs in 1 M KOH. (b) Overall water splitting performance of NiCo LDH-V_{Ni}/CC||NiCo LDH-V_{Ni}/CC and Pt/C||IrO_2 electrode pairs in 1 M KOH.

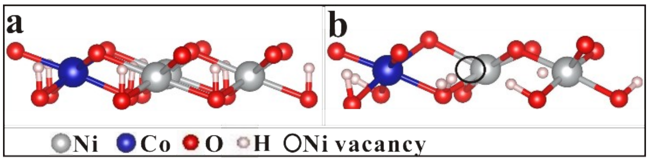

Fig. S16. Side-view schematic models of (a) NiCo LDH and (b) NiCo LDH-V_{Ni}.

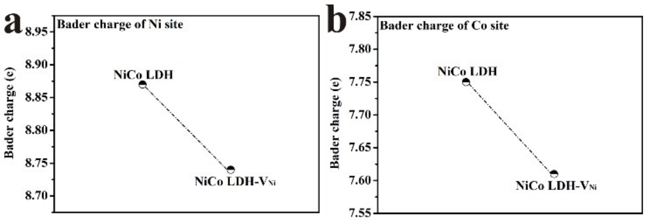

Fig. S17. Bader charge analysis around the Ni vacancies of the (a) Ni sites and (b) Co sites on NiCo LDH and NiCo LDH-V_{Ni}.

Table S1. Comparison of the HER performance of NiCo LDH-V_{Ni}/CC with other reported catalysts in 1 M KOH.

Catalysts	**Overpotential at 10 mA cm^{-2} (mV)**	**Tafel slope (mV dec^{-1})**	**References**
NiCo LDH-V_{Ni}/CC	**195**	**135**	**This work**
B-Co LDH/NF	236	92	[4]
NiCo-LDH/$NiCo_2S_4$/CC	219	41	[5]
NiFe LDH/NF	365	151	[6]
CoV LDH/NF	248	134.8	[7]
Cu_2MoS_4-MoS_2/NSG	238.1	67.5	[8]
Co_4S_3/CC	406	164	[9]
NiCo-LDH/NF	248	124.8	[10]
NiCo-LDH@CdS	225	76	[11]

Table S2. Comparison of the OER performance of NiCo LDH-V_{Ni}/CC with other reported catalysts in 1 M KOH.

Catalysts	**Overpotential at 10 mA cm^{-2} (mV)**	**Tafel slope (mV dec^{-1})**	**References**
NiCo LDH-V_{Ni}/CC	**227**	**67**	**This work**
NiCo-LDHs/Ar/CC	299	45	[12]

CuO/NiCo-LDH	262	49.36	13
NiCo-LDH/CFP	299	80	14
NiCo-LDH/NiCo$_2$S$_4$/CC	254	48	5
Ir/NiCo LDH	210	47	15
Co-LDH/ZIF-67	246	102	16
CoV LDH/NF	318	111.4	7
NiCo-LDH/NF	257	88.3	10

References

1 B. Wei, Z. Fu, D. Legut, T. C. Germann, S. Du, H. Zhang, J. S. Francisco, R. Zhang, *Adv. Mater.*, 2021, **33**, 2102595.

2 Z. Tang, S. Zhao, Y. Yang, *Angew. Chem. Int. Ed.*, 2021, **61**, 202110186.

3 A. Liu, X. Liang, X. Ren, W. Guan, M. Gao, Y. Yang, Q. Yang, L. Gao, Y. Li, T. Ma, *Adv. Funct. Mater.*, 2020, **30**, 2003437

4. H. Yang, Z. Chen, P. Guo, B. Fei and R. Wu, *Appl. Catal. B.*, 2020, **261**, 118240.
5. Y. Liu, Y. Bai, W. Yang, J. Ma and K. Sun, *Electrochim. Acta*, 2021, **367**, 137534.
6. B. R. Wang, S. Jiao, Z. Wang, M. Lu, D.Chen, Y. Kang, G. Pang, S. Feng, *J. Mater. Chem. A*, 2020, **8**, 17202-17211.
7. W. Li, B. Feng, L. Yi, J. Li, W. Hu, *ChemSusChem*, 2021, **14**, 730-737.
8. D. C. Nguyen, D. T. Tran, T. Doan, D. H. Kim, N. H. Kim, J. H. Lee, *Adv. Energy Mater.*, 2020, **10**, 1903289.
9. X. Zang, X. Zhang, J. Guo, *Mater. Lett.*, 2020, **285**, 129057.
10. L. Zhang, J. Peng, Y. Yuan, W. Zhang, K. Peng, *Appl. Surf. Sci.*, 2021, **557**, 118-130.
11. A. Pirkarami, S. Rasouli, E. Ghasemi, *J. Energy Chem.*, 021, **57**, 118-130.
12. Y. Liu, M. Zhang, D. Hu, R. Li, K. Hu, K.Yan, *ACS Appl. Energy Mater.*, 2019, **2**, 1162-1168..
13. B. Chen, Z. Zhang, S. Kim, M. Baek and K. Yong, *Appl. Catal. B*, 2019, **259**, 118017.

14. X. Han, Y. Niu, C. Yu, Z. Liu, H. Huang, H. Huang, S. Li, W. Guo, X. Tan, J. Qiu, *Nano Energy*, 2019, **69**, 104367.
15. R. Fan, Q. Mu, Z. Wei, Y. Peng, M. Shen, *J. Mater. Chem. A*, 2020, **8**, 9871-9881.
16. Z. Li, X. Zhang, Y. Kang, C. Yu, Y. Wen, M. Hu, D. Meng, W. Song, Y. Yang, *Adv. Sci*. 2020, **8**, 2002631